



## Optical, structural, and functional properties of highly reflective and stable iridium mirror coatings for infrared applications: supplement

PAUL SCHMITT,<sup>1,2</sup>  NADJA FELDE,<sup>1</sup> THORSTEN DÖHRING,<sup>3</sup>  
MANFRED STOLLENWERK,<sup>3</sup> INGO USCHMANN,<sup>4</sup> KEVIN HANEMANN,<sup>1</sup>  
MARIE SIEGLER,<sup>1</sup> GEORG KLEMM,<sup>1</sup> NANCY GRATZKE,<sup>1</sup> ANDREAS  
TÜNNERMANN,<sup>1,2</sup> STEFAN SCHWINDE,<sup>1</sup> SVEN SCHRÖDER,<sup>1</sup> AND  
ADRIANA SZEGHALMI<sup>1,2,\*</sup> 

<sup>1</sup>Fraunhofer Institute for Applied Optics and Precision Engineering IOF, Center of Excellence in Photonics, Albert-Einstein-Str. 7, D-07745 Jena, Germany

<sup>2</sup>Friedrich Schiller University Jena, Faculty of Physics and Astronomy, Institute of Applied Physics IAP, Albert-Einstein-Str. 15, D-07745 Jena, Germany

<sup>3</sup>TH Aschaffenburg - University of Applied Sciences, Würzburger Str. 45, D-63743 Aschaffenburg, Germany

<sup>4</sup>Friedrich Schiller University Jena, Faculty of Physics and Astronomy, Institute of Optics and Quantum Electronics IOQ, Max-Wien-Platz 1, D-07743 Jena, Germany

\*[a.szeghalmi@uni-jena.de](mailto:a.szeghalmi@uni-jena.de)

---

This supplement published with Optica Publishing Group on 13 January 2022 by The Authors under the terms of the [Creative Commons Attribution 4.0 License](https://creativecommons.org/licenses/by/4.0/) in the format provided by the authors and unedited. Further distribution of this work must maintain attribution to the author(s) and the published article's title, journal citation, and DOI.

Supplement DOI: <https://doi.org/10.6084/m9.figshare.17121509>

Parent Article DOI: <https://doi.org/10.1364/OME.447306>

# Optical, structural, and functional properties of highly reflective and stable iridium mirror coatings for infrared applications: supplemental document

Highly reflective and stable iridium (Ir) mirror coatings were fabricated by atomic layer deposition (ALD) and magnetron sputtering (MS). In Fig. S1, atomic force microscopy (AFM) images for  $1 \times 1 \mu\text{m}^2$  and  $10 \times 10 \mu\text{m}^2$  measurement areas demonstrate that the Ir MS surface is significantly smoother compared to Ir ALD. Nevertheless, the maximum scatter-induced reflectance losses [1] with  $< 0.15 \%$  are negligible in the IR spectral range.

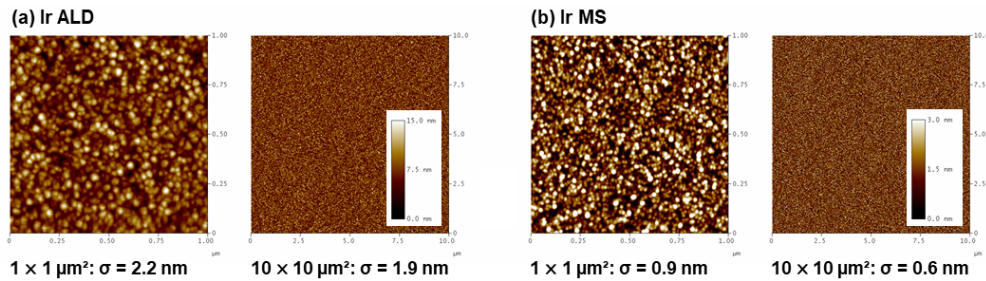


**Fig. S1.** Atomic force microscopy (AFM) images of iridium coatings fabricated by (a) atomic layer deposition (ALD) and (b) magnetron sputtering (MS) for  $1 \times 1 \mu\text{m}^2$  and  $10 \times 10 \mu\text{m}^2$  measurement areas. For all images, the calculated root-mean-square (rms) surface roughness is given. The Ir MS surface is significantly smoother compared to Ir ALD, with the color scale valid for both measurement areas.

The top-view scanning electron microscopy (SEM) images in Fig. S2 illustrate the topography differences of Ir ALD and Ir MS. For the Ir ALD coating, the grains on the surface exhibit an elongation of about 18 - 45 nm. The Ir MS grains with about 13 - 25 nm elongation are significantly smaller compared to Ir ALD, as confirmed by X-ray diffraction (XRD) analysis. In addition, the Ir MS surface appears significantly smoother, as confirmed by AFM.

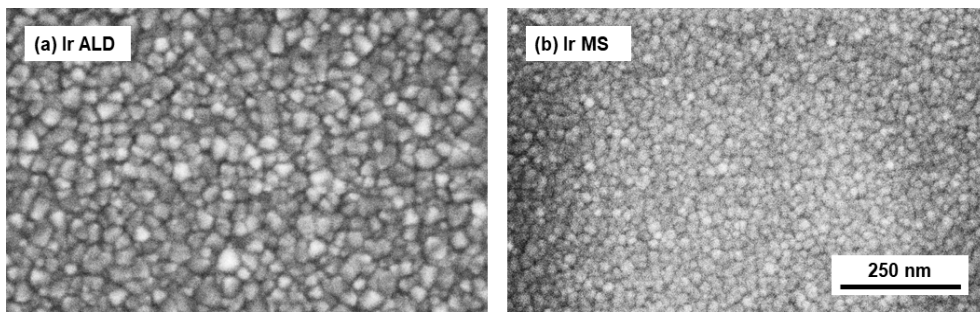


**Fig. S2.** Top-view scanning electron microscopy (SEM) images of (a) Ir ALD and (b) Ir MS coatings. The Ir MS grains on the surface are significantly smaller compared to Ir ALD, as confirmed by X-ray diffraction (XRD) analysis. The scale bar in the bottom right corner is valid for both SEM images.

The optical constants of the Ir coatings were evaluated by multi-experiments combining spectrophotometry (SP), Fourier-transform infrared spectroscopy (FTIR) in reflection mode, and variable-angle spectroscopic ellipsometry (SE) measurements in the wavelength range from 200 nm to 20  $\mu\text{m}$ . By using the SpetraRay/4 (Sentech Instruments, Germany) software

package, a Drude-Lorentz model with five Lorentz oscillators and effective-medium-approximation (EMA) top layer, according to the Bruggeman approach, was applied. The fixed thickness of the EMA layer, consisting of 50 % voids and 50 % Ir, equals the Ir surface roughness as determined by AFM ( $1 \times 1 \mu\text{m}^2$ ) measurements. Only the ( $2 + 2 + 3 \times 5 = 19$ ) Drude-Lorentz parameters were fitted. The corresponding complex dielectric function  $\varepsilon(\omega)$  is given by Eq. (S1) [2,3]:

$$\varepsilon(\omega) = \varepsilon_\infty - \frac{\omega_p^2}{\omega^2 - i\omega\Gamma_D} + \sum_{j=1}^5 \frac{f_j \omega_{0j}^2}{\omega_{0j}^2 - \omega^2 - i\omega\Gamma_j}, \quad (\text{S1})$$

with  $\omega = 2\pi c/\lambda$  being the angular frequency and  $c$  being the speed of light. Drude absorption of free charge carriers includes two parameters: the plasma frequency  $\omega_p$  and damping factor  $\Gamma_D$ . The Lorentz model uses two parameters (real and imaginary part) for the complex background constant  $\varepsilon_\infty$  and three parameters for each oscillator  $j$ : center frequency  $\omega_{0j}$ , strength  $f_j$ , and damping factor  $\Gamma_j$ . In Fig. S3, the experimental and fitted data for the Ir MS coating are presented with a mean-squared-error (MSE) value below 0.30.

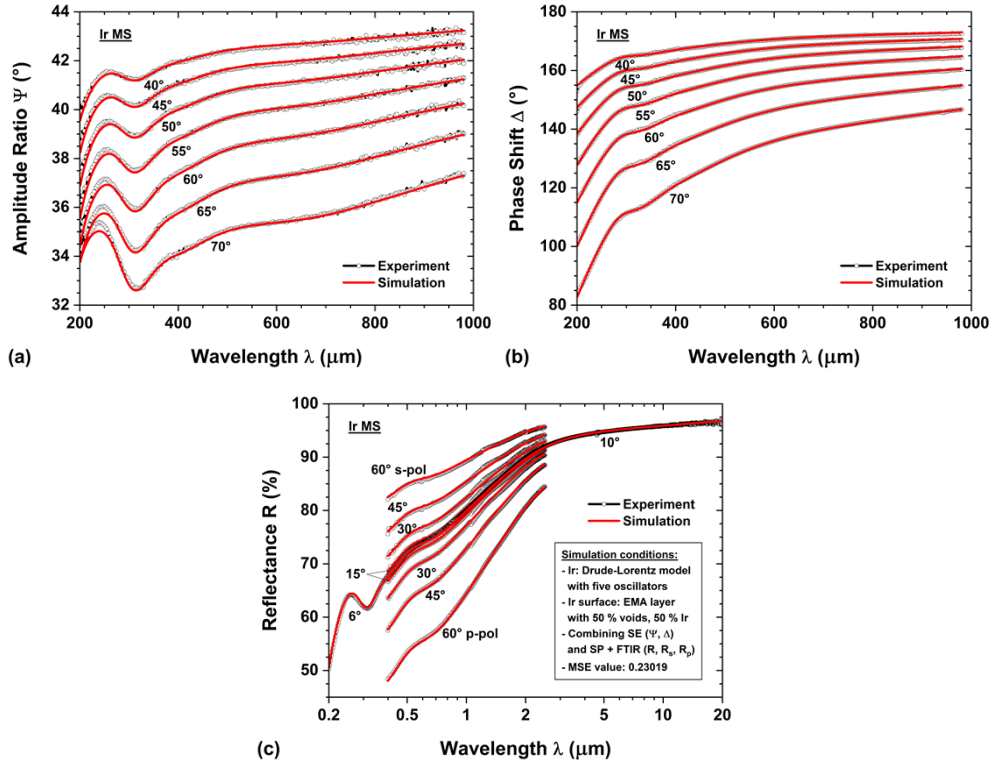


**Fig. S3.** For the Ir MS coating, the experimental (black) and fitted (red) data of the (a) ellipsometric amplitude ratio, (b) ellipsometric phase shift, and (c) specular reflectance are shown, using a Drude-Lorentz model with five Lorentz oscillators and effective-medium-approximation (EMA) top layer, according to the Bruggeman approach.

The evaluated optical constants, meaning the refractive index  $n$  and extinction coefficient  $k$ , of the Ir ALD and Ir MS coatings are listed in Table S1 at selected wavelengths and corresponding photon energies, shown in Fig. 3 in the article, and publicly available under [4].

**Table S1. Optical constants of Ir coatings fabricated by ALD and MS at selected wavelengths.<sup>a</sup>**

Wavelength $\lambda$ ( $\mu\text{m}$ )	Photon Energy E (eV)	Ir ALD		Ir MS	
		n	k	n	k
0.200	6.200	0.93	1.91	0.98	2.04
0.220	5.641	0.92	2.30	0.99	2.40
0.240	5.175	1.00	2.69	1.09	2.75
0.259	4.780	1.19	3.05	1.27	3.07
0.279	4.441	1.49	3.30	1.53	3.28
0.299	4.146	1.76	3.33	1.75	3.34
0.319	3.889	1.81	3.31	1.81	3.37
0.339	3.661	1.76	3.41	1.82	3.48
0.358	3.459	1.76	3.62	1.85	3.65
0.378	3.278	1.83	3.83	1.91	3.83
0.398	3.115	1.93	4.00	1.99	3.99
0.448	2.770	2.11	4.36	2.17	4.37
0.497	2.494	2.31	4.75	2.37	4.75
0.557	2.228	2.61	5.13	2.66	5.15
0.606	2.046	2.83	5.39	2.90	5.42
0.656	1.891	3.01	5.60	3.09	5.65
0.705	1.758	3.14	5.79	3.24	5.86
0.755	1.643	3.24	5.99	3.36	6.08
0.804	1.542	3.30	6.21	3.46	6.31
0.854	1.452	3.35	6.44	3.56	6.55
0.903	1.373	3.40	6.69	3.64	6.79
0.953	1.301	3.44	6.95	3.73	7.04
1.002	1.237	3.50	7.22	3.80	7.28
1.507	0.8226	3.93	9.72	4.45	9.90
2.003	0.6192	3.75	12.58	5.07	12.65
2.498	0.4964	3.91	15.99	5.86	15.47
3.003	0.4129	4.52	19.50	6.88	18.28
3.498	0.3545	5.42	22.83	8.07	20.90
4.004	0.3097	6.53	26.07	9.40	23.40
4.509	0.2750	7.80	29.14	10.83	25.72
5.004	0.2478	9.14	32.00	12.27	27.82
6.004	0.2065	12.07	37.34	15.22	31.61
7.005	0.1770	15.18	42.14	18.13	34.89
8.005	0.1549	18.35	46.45	20.93	37.76
9.006	0.1377	21.52	50.35	23.59	40.31
10.006	0.1239	24.64	53.89	26.11	42.62
11.006	0.1127	27.70	57.11	28.50	44.73
12.007	0.1033	30.66	60.08	30.77	46.69
13.007	0.0953	33.52	62.83	32.93	48.51
14.008	0.0885	36.29	65.38	34.98	50.23
15.008	0.0826	38.96	67.78	36.94	51.87
16.008	0.0775	41.53	70.04	38.82	53.42
17.009	0.0729	44.02	72.17	40.62	54.92
18.009	0.0689	46.42	74.20	42.35	56.35
19.000	0.0653	48.71	76.13	44.01	57.72
20.000	0.0620	50.96	77.99	45.62	59.07

<sup>a</sup>Note: The high-resolution optical constants for iridium are publicly available under [www.refractiveindex.info](http://www.refractiveindex.info) [4].

The protected Ag mirror coatings failed the climate stability (#2) and H<sub>2</sub>O solubility (#3) tests sequences. After the final adhesion tests, the Ag mirrors show delamination of their protective layers, as Fig. S4 illustrates. Additionally, reddish and reddish-purple discolorations were visible by the unaided eye after the climatic stability and H<sub>2</sub>O solubility test sequences, respectively.

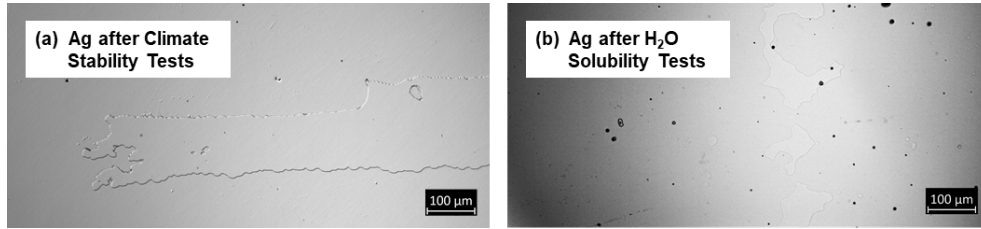


**Fig. S4.** Microscope images (top-view) of protected Ag mirror coatings after the (a) climate stability and (b) H<sub>2</sub>O solubility test sequences. After the final adhesion tests, delamination and discoloration were visible.

After annealing at 600 °C, the Ir coatings deposited on fused silica (FS) show reflectance losses, as Fig. S5 illustrates. The surface of the Ir ALD coating appears milky, resulting in minor specular reflectance losses of 0.5 - 2.2 % between 200 nm and 1.2 μm. However, Ir ALD shows a slightly higher reflectance for wavelengths  $\geq 2$  μm upon annealing at 600 °C. The Ir MS reflectance on both Si wafers and FS decreases by 7.6 % in the IR spectral range compared to the unannealed coating. XRD analysis indicates an intermixing of the Ir and Cr adhesion layer.

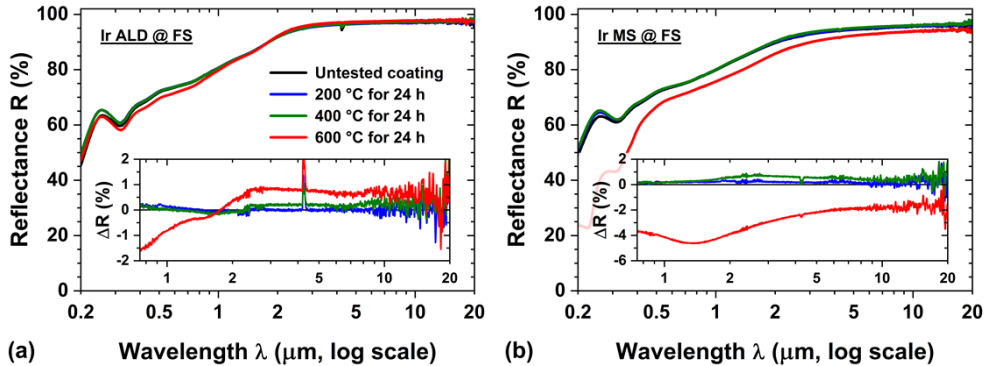


**Fig. S5.** Specular reflectance of unprotected (a) Ir ALD and (b) Ir MS coatings deposited on fused silica (FS) after thermal stability tests. The insets illustrate the reflectance changes after annealing for 24 h at 200 °C (blue), 400 °C (green), and 600 °C (red) compared to the untested coating (black).

## References

1. H. E. Bennett and J. O. Porteus, "Relation Between Surface Roughness and Specular Reflectance at Normal Incidence," *J. Opt. Soc. Am.* **51**, 123–129 (1961).
2. O. Stenzel, *Optical Coatings. Material Aspects in Theory and Practice* (Springer-Verlag, 2014).
3. J. Jaiswal, S. Mourya, G. Malik, S. Chauhan, A. Sanger, R. Daipuriya, M. Singh, and R. Chandra, "Determination of optical constants including surface characteristics of optically thick nanostructured Ti films: analyzed by spectroscopic ellipsometry," *Appl. Opt.* **55**, 8368–8375 (2016).
4. M. N. Polyanskiy, "Refractive index database," <https://refractiveindex.info>. Accessed on 2021-10-28.